

## Population Pharmacokinetics of Ethambutol in South African Tuberculosis Patients<sup>∇</sup>

Siv Jönsson,<sup>2\*</sup> Alistair Davidse,<sup>1</sup> Justin Wilkins,<sup>1,2†</sup> Jan-Stefan Van der Walt,<sup>1,2</sup>  
Ulrika S. H. Simonsson,<sup>2</sup> Mats O. Karlsson,<sup>2</sup> Peter Smith,<sup>1</sup>  
and Helen McIlleron<sup>1</sup>

*Division of Clinical Pharmacology, Department of Medicine, University of Cape Town, Cape Town, South Africa,<sup>1</sup> and  
Department of Pharmaceutical Biosciences, Uppsala University, Uppsala, Sweden<sup>2</sup>*

Received 28 February 2011/Returned for modification 7 April 2011/Accepted 8 June 2011

**Ethambutol, one of four drugs in the first-line antitubercular regimen, is used to protect against rifampin resistance in the event of preexisting resistance to isoniazid. The population pharmacokinetics of ethambutol in South African patients with pulmonary tuberculosis were characterized using nonlinear mixed-effects modeling. Patients from 2 centers were treated with ethambutol (800 to 1,500 mg daily) combined with standard antitubercular medication. Plasma concentrations of ethambutol were measured following multiple doses at steady state and were determined using a validated high-pressure liquid chromatography-tandem mass spectrometric method. The data comprised 189 patients (54% male, 12% HIV positive) weighing 47 kg, on average (range, 29 to 86 kg), and having a mean age of 36 years (range, 16 to 72 years). The estimated creatinine clearance was 79 ml/min (range, 23 to 150 ml/min). A two-compartment model with one transit compartment prior to first-order absorption and allometric scaling by body weight on clearance and volume terms was selected. HIV infection was associated with a 15% reduction in bioavailability. Renal function was not related to ethambutol clearance in this cohort. Interoccasion variability exceeded interindividual variability for oral clearance (coefficient of variation, 36 versus 20%). Typical oral clearance in this analysis (39.9 liters/h for a 50-kg individual) was lower than that previously reported, a finding partly explained by the differences in body weight between the studied populations. In summary, a population model describing the pharmacokinetics of ethambutol in South African tuberculosis patients was developed, but additional studies are needed to characterize the effects of renal function.**

In order to optimize treatment regimens, there is an urgent need to critically evaluate the pharmacokinetics and corresponding effects of the antitubercular drugs among patients with tuberculosis. Population pharmacokinetic modeling is considered an efficient means to summarize data in terms of typical parameter estimates, effects of covariates (e.g., body weight, sex, and gender), and unexplained variability. Furthermore, population pharmacokinetic models are valuable for simulation purposes and enable alternative dose regimens for subpopulations aiming at specific pharmacokinetic target levels to be assessed to establish more effective treatment. The present analysis was designed to describe the population pharmacokinetics of ethambutol (EMB) in a South African patient population, including the characterization of interindividual variability (IIV) and interoccasion variability (IOV) and exploration of the causes of variability, which have not been addressed in previous models (27, 39).

EMB is a bacteriostatic agent with a mechanism of action that has been suggested to occur by inhibition of mycobacterial cell wall synthesis. The primary role of EMB in the first-line four-drug antitubercular regimen (i.e., EMB in combination with rifampin, isoniazid, and pyrazinamide) is to protect

against rifampin resistance in the event of preexisting resistance to isoniazid (2, 38). One well-known adverse effect relates to impairment of visual acuity and color vision in one or both eyes as a result of dose-dependent optic neuritis, but ocular toxicity is rare when EMB is used for 2 to 3 months at recommended doses (38).

EMB has been reported to have an oral bioavailability of approximately 80%, and concomitant food intake decreases the rate of absorption but not the extent of absorption (1, 27). EMB is eliminated mainly via renal filtration and active tubular secretion; approximately 50 to 70% and 70 to 84% of oral and intravenous doses, respectively, are recovered unchanged in the urine of subjects with normal renal function (6, 18, 19, 25). EMB has a low plasma protein binding, with an unbound fraction of 70 to 80% (18). The systemic concentrations of EMB in tuberculosis patients have been described previously (7, 13, 22, 28, 30, 39). However, population pharmacokinetic models have been developed only on the basis of data from healthy volunteers (27) and data from North American tuberculosis patients (39).

### MATERIALS AND METHODS

**Patients.** The data from two prospective pharmacokinetic studies performed at DP Marais SANTA Centre near Cape Town, South Africa, and Brewelskloof Hospital near Worcester, South Africa, among patients diagnosed with pulmonary tuberculosis were pooled in this analysis. The study at DP Marais SANTA Centre was specifically designed to investigate pharmacokinetics, while the Brewelskloof Hospital study also aimed at studying short- and medium-term treatment outcomes, in addition to pharmacokinetics. Patients at both hospitals were inpatients admitted for reasons that included a poor response to treatment,

\* Corresponding author. Mailing address: Department of Pharmaceutical Biosciences, Uppsala University, P.O. Box 591, SE-751 24 Uppsala, Sweden. Phone: 46 18 471 40 00. Fax: 46 18 471 40 03. E-mail: siv.jonsson@farmbio.uu.se.

† Present address: Exprimo NV, Mechelen, Belgium.

∇ Published ahead of print on 20 June 2011.

suspected nonadherence, debility, severe or complicated disease, and poor socioeconomic circumstances. A population analysis approach was planned for the DP Marais SANTA Centre study prospectively, and merging of the data from the two pharmacokinetic studies resulted in a larger data set, which provided advantages in searching for covariate relationships and more precisely estimating the values of population pharmacokinetic parameters. A traditional pharmacokinetic analysis of the data from the Brewelskloof Hospital has been reported previously (22).

EMB was administered to 60 patients enrolled in the study performed at the DP Marais SANTA Centre in combination with isoniazid, pyrazinamide, rifampin, and, for some patients, streptomycin at doses prescribed by the attending physician. EMB was administered at doses of 800 to 1,200 mg once daily five times a week, with drug holidays on Saturdays and Sundays. Patients were sampled over a 2-week period on four occasions at least 2 weeks after the start of therapy. On each occasion three samples were taken at random times between 0 and 12 h postdose. Sampling usually occurred on Tuesdays and Fridays, with a few patients being sampled on Mondays and Thursdays.

One hundred twenty-nine patients enrolled in the study at the Brewelskloof Hospital received oral doses of EMB daily (800 to 1,500 mg EMB) as part of their standard antitubercular medication, as prescribed by hospital staff. There were no drug holidays. Patients were sampled predose and at 0.5, 1, 1.5, 2, 2.5, 3, 4, 6, and 8 h postdose on a single occasion 2 months after admission.

The drug products used were those routinely administered in the hospital and comprised ethambutol as Purderal (400-mg tablet; Pharmicare Ltd.), ethambutol as Rolab (400-mg tablet; Rolab [Pty.] Ltd.), and a Rifafour e-275 tablet (fixed-dose combination of rifampin-isoniazid-pyrazinamide-ethambutol at 150/75/400/275 mg; Sanofi-Aventis). All formulations were approved for use by the Medicines Control Council of South Africa.

Both studies were performed in accordance with the Declaration of Helsinki and approved by the University of Cape Town's Faculty of Health Sciences Research Ethics Committee, South Africa, as well as the corresponding counterpart bodies at the participating study centers. Each patient provided full written informed consent.

**Dose intake and sample collection.** All patients fasted from 10 p.m. on the evenings prior to blood sampling. Ingestion of medication was carefully monitored by a member of the study team. Patients were not permitted to ingest food or water for a period of 2 h after the dose.

Blood samples were placed on ice before centrifugation at room temperature. Plasma samples (at least 1.2 ml) were stored at  $-80^{\circ}\text{C}$  within 30 min of sample collection. Serum chemistry (alkaline phosphatase, alanine aminotransferase, aspartate aminotransferase, serum creatinine, total bilirubin, and urea levels) and complete blood cell count (hemoglobin and hematocrit levels, red blood cell count, mean corpuscular volume, and white blood cell count) were determined and investigated as potential covariates.

**Drug quantification.** Total EMB concentrations in plasma (plasma protein bound plus unbound) were determined using a previously published high-pressure liquid chromatography–tandem mass spectrometric method with some modifications (9). The method was validated over the concentration range of 0.1 to 10 mg/liter. At concentrations of 0.15, 0.45, and 1.5 mg/liter, rates of recovery were 93.3, 90.0, and 85.7%, respectively. Intraday accuracies at the same concentrations were 102.9, 95.0, and 92.3% with precisions of 5.2, 3.4, and 2.1%. Corresponding interday accuracies were 103.1, 96.9, and 94.2% with precisions of 4.7, 5.35, and 4.0%. No interference from isoniazid, pyrazinamide, or rifampin was observed.

Drug concentrations below the lower limit of the validated range were excluded in the pharmacokinetic analysis. This approach is not expected to result in appreciable bias in parameter estimates since these samples contributed by less than 2% ( $n = 35$ ) to the total number of samples.

**Pharmacokinetic analysis.** Model building was performed using the NONMEM program, version VI (4). The first-order conditional estimation method with interaction was used to estimate population pharmacokinetic parameters. The Xpose program (version 4.2.1 [http://xpose.sourceforge.net, accessed 20 September 2010]) managed the processes of model building and data analysis (14).

The NONMEM data set was constructed to take into account the actual dose regimens and actual time points for sampling.

Single-compartment and multicompartment models with first-order absorption and elimination were fitted to log-transformed data. Different approaches for the modeling of the absorption were tested, including the use of a lag time and of transit compartments (31, 36). Interindividual variability was evaluated for all pharmacokinetic parameters, and interoccasion variability was evaluated for oral clearance ( $CL/F$ ; where  $F$  is the bioavailability term) (15). Log-normal

distributions were employed as exemplified for  $CL/F$ :  $(CL/F)_{ij} = TV(CL/F) \cdot \exp(\eta_i + \kappa_{ij})$ , where  $CL/F_{ij}$  is the oral clearance for the  $i$ th individual at the  $j$ th occasion,  $TV(CL/F)$  is the typical value of clearance in the population, and  $\eta_i$  and  $\kappa_{ij}$  are random variables assumed to be normally distributed with mean 0 and variance  $\omega^2$  and variance  $\pi^2$ , respectively. While  $\eta_i$  describes the difference between the  $i$ th individual's oral clearance and the typical value for the population,  $\kappa_{ij}$  describes the differences in the  $i$ th individual's oral clearance arising from the different sampling occasions. Residual variability was described with both additive and proportional error terms.

Selection between nested models was performed using the NONMEM objective function value (OFV) in the likelihood ratio test. The difference in OFV between a full and a reduced model is approximately  $\chi^2$  distributed, and a decrease of  $\geq 3.84$  corresponds to a significance level of  $\leq 0.05$ .

Following development of a basic structural model, the covariate model building was performed, but owing to very long run times, a simple absorption model (a model with first-order absorption and a lag time) was used as the basic model. Relationships identified with this approach were eventually rechallenge using the final structural model. Initially, allometric scaling by body weight was introduced on all clearance and volume terms with powers of 3/4 and 1, respectively (3, 34, 35). Thereafter, the statistical significance for the following covariates on  $CL/F$  was tested one at a time within NONMEM: body weight, age, all serum chemistry and blood cell count variables, estimated creatinine clearance according to the Cockcroft and Gault method (8) truncated at 150 ml/min, sex, race, alcohol use prior to admission, location of study, and dose. Dose was tested as a categorical covariate using the actual total dose administered, and dose/kg body weight was included as a continuous covariate. Body mass index (BMI), lean body weight (LBW), height, and body surface area were highly correlated with body weight ( $r \geq 0.8$ ), and for practical reasons, body weight was used as the measure for body size in the covariate testing. Covariate values were obtained at the time of the first pharmacokinetic sampling unless stated otherwise. The statistically significant relationships ( $P < 0.05$ ) were subject to a stepwise forward addition into the model (significance level, 0.05), followed by a backwards deletion (significance level, 0.001). The stepwise covariate model building (*scm*) procedure in Perl-speaks-NONMEM (version 3.0.0 [http://psn.sourceforge.net/, accessed 20 September 2010]) was used for this task (20, 21). For the univariate search and the *scm* procedure, the data set was randomly split (stratified by location) to produce two equally sized data sets, one of which was used for the forward step and the other of which was used for the backward step. Following completion of the *scm* procedure, the model parameters were reestimated for the complete data set. In accordance with prior knowledge (22, 39), the effect of the presence of HIV on bioavailability was eventually evaluated.

Imprecision in parameter estimates was assessed using output obtained from NONMEM and by application of nonparametric bootstrapping (200 replicates, using random sampling with replacement). A visual predictive check (VPC) with population prediction correction (1,000 replicates) was used to assess the capability of the final model to reflect the observed data (5, 12, 16). Eta (interindividual variability) and epsilon (residual error) shrinkages were calculated as described by Savic and Karlsson (32) to allow an assessment of the quality of diagnostics on the basis of empirical Bayes estimates. Perl-speaks-NONMEM (versions 3.2.10 and 3.2.12 [http://psn.sourceforge.net/, accessed 20 September 2010]) was employed to perform the bootstrap, VPC, and shrinkage calculations (20, 21).

To compare how well previous models fit the data, model predictions of the present data were made by applying the previously published population models (27, 39) in a VPC (200 replicates). The previous models were obtained by means of nonparametric estimation methods, and therefore, the variability models from our model were employed in the VPCs. In addition, in a second step the models were modified by introducing allometric scaling by body weight on all volume and clearance terms (power terms set to 1 and 3/4, respectively).

## RESULTS

In total, 1,869 pharmacokinetic observations from 189 patients were included in the analysis, and the observed data are given in Fig. 1. Patient characteristics and the daily dose administered are presented in Table 1. Demographics (including serum chemistry and blood cell count) were largely similar at the two sites. Some of the characteristics were statistically significantly different ( $P < 0.05$ ) between the sites, but the magnitudes of the differences were relatively small (Table 1).

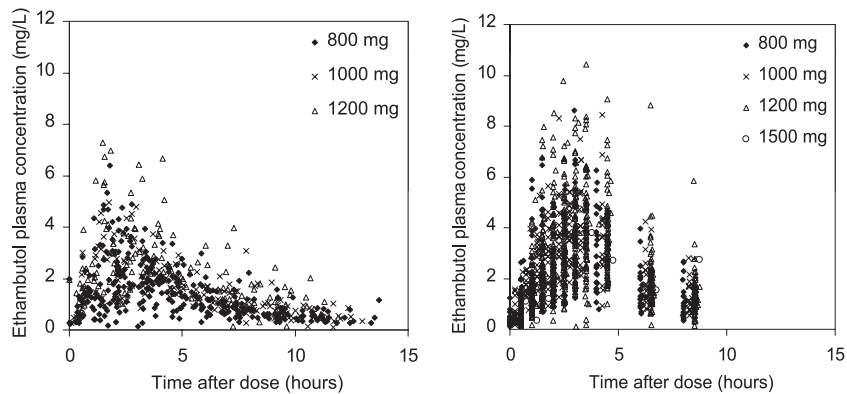


FIG. 1. Observed concentrations obtained in patients at DP Marais SANTA Centre (left) and Brewelskloof Hospital (right). At DP Marais SANTA Centre, dosing occurred Monday to Friday, whereas the dosing was daily at Brewelskloof Hospital. In the right panel, the time points for each dose level are shifted to the right to better see the data from the four dose levels.

Of note is that the proportion of patients with malnutrition is large: 18% had BMIs of  $<16 \text{ kg/m}^2$  (severe malnutrition), and of the whole sample studied, 47% can be classified as not having malnutrition; i.e., BMIs were  $\geq 18.5 \text{ kg/m}^2$ .

The plasma concentrations of EMB were best described by a two-compartment model with one transit compartment prior to absorption and first-order elimination. Only two covariates were found to influence the systemic exposure of EMB: body

TABLE 1. Patient characteristics and daily dose of ethambutol

	DP Marais SANTA Centre	Brewelskloof Hospital	Combined
No. of subjects	60	129	189
Median (range) age (yr)	38 (18–64)	36 (16–72)	36 (16–72)
Median (range) wt (kg) <sup>a</sup>	52 (36–67)	46 (29–86)	47 (29–86)
Median (range) BMI ( $\text{kg/m}^2$ ) <sup>a,b</sup>	19 (15–23)	18 (12–36)	18 (12–36)
Median (range) serum creatinine level ( $\mu\text{mol/liter}$ )	77 (48–121)	74 (43–174)	74 (43–174)
Median (range) creatinine clearance ( $\text{ml/min}$ ) <sup>c</sup>	80 (51–150)	78 (23–128)	79 (23–150)
Median (range) alkaline phosphatase concn (U/liter) <sup>a</sup>	87 (53–619)	73 (39–276)	77 (39–619)
Median (range) alanine aminotransferase concn (U/liter)	18 (8.0–57)	15 (6.0–58)	16 (6.0–58)
Median (range) aspartate aminotransferase concn (U/liter) <sup>a</sup>	26 (11–94)	18 (9.0–63)	22 (9.0–94)
Median (range) total bilirubin concn ( $\mu\text{mol/liter}$ )	6.0 (1.0–13)	6.0 (1.0–33)	6.0 (1.0–33)
Median (range) urea concn (mmol/liter)	3.7 (2.1–8.5)	3.3 (1.9–13)	3.5 (1.9–13)
Median (range) serum hemoglobin concn (g/dl)	12 (8.2–16)	12 (7.4–15)	12 (7.4–16)
Median (range) hematocrit (%)	37 (25–49)	38 (24–47)	38 (24–49)
Median (range) mean corpuscular vol (fl) <sup>a</sup>	89 (72–102)	93 (62–121)	91 (62–121)
Median (range) red blood cell count ( $10^{12}/\text{liter}$ )	4.2 (2.6–5.8)	4.2 (2.2–5.7)	4.2 (2.2–5.8)
Median (range) white blood cell count ( $10^9/\text{liter}$ ) <sup>a</sup>	6.8 (1.1–17)	8.4 (3.4–26)	7.9 (1.1–26)
No. (%) of subjects by sex <sup>a</sup>			
Male	45 (75)	57 (44)	102 (54)
Female	15 (25)	72 (56)	87 (46)
No. (%) of subjects by race <sup>a,d</sup>			
Black	15 (25)	15 (12)	30 (16)
Colored	43 (72)	113 (88)	156 (83)
White	2 (3)	0 (0)	2 (1)
No. (%) of subjects with moderate to high alcohol use <sup>a</sup>	47 (78)	78 (60)	125 (66)
No. (%) of subjects HIV positive	12 (20)	12 (9.3)	24 (13)
No. (%) of subjects receiving daily ethambutol dose (mg) of:			
800	31 (52)	23 (18)	54 (29)
1,000	15 (25)	18 (14)	33 (17)
1,200	14 (23)	87 (67)	101 (53)
1,500	0 (0)	1 (1)	1 (1)

<sup>a</sup> Statistically significant difference between sites at the 95% confidence level.

<sup>b</sup> For the DP Marais SANTA Centre, Brewelskloof Hospital, and combined groups, 5%, 24%, and 18% of the patients, respectively, had BMIs of  $<16 \text{ kg/m}^2$ .

<sup>c</sup> Distribution truncated at 150 ml/min.

<sup>d</sup> With respect to race, the proportions of blacks were compared between the two locations.

TABLE 2. Final parameter estimates by NONMEM, together with bootstrap estimates presented as medians

Parameter <sup>a</sup>	NONMEM value/bootstrap value <sup>b</sup>	
	Estimate	% relative SE <sup>c</sup>
$k_a$ (h <sup>-1</sup> )	0.474/0.498	24/19
IIV on $k_a$ (% CV)	39 <sup>d</sup> /43	80/61
MTT (h)	0.789/0.770	17/18
IIV on MTT (% CV)	93 <sup>e</sup> /90	20/22
Effect of presence of HIV on $F$ (fractional change)	-0.154/-0.162	40/39
CL/ $F$ (liter/h)	39.9/39.7	3.1/5.9
IIV on CL/ $F$ (% CV)	20 <sup>f</sup> /21	57/86
IOV on CL/ $F$ (% CV)	36/34	45/87
$V_1$ / $F$ (liters)	82.4/90.0	42/29
$V_2$ / $F$ (liters)	623/642 <sup>g</sup>	22/30 <sup>g</sup>
$Q$ (liters/h)	34.3/33.8	10/7.9
Additive residual error (mg/liter)	0.107/0.104	20/29
Proportional residual error (% CV)	31.8/31.6	4.4/4.6

<sup>a</sup>  $k_a$ , absorption rate constant; MTT, mean transit time;  $V_1$ / $F$ , central volume of distribution;  $V_2$ / $F$ , peripheral volume of distribution;  $Q$ , intercompartmental clearance; CV, coefficient of variation. Typical value of  $F = 1 \cdot (1 - 0.154 \times \text{HIV})$ , with HIV being 0 and 1 for negative and positive HIV status, respectively; typical value of CL/ $F = 39.7 \cdot (\text{body weight}/50)^{3/4}$ ; typical value of central volume of distribution =  $82.4 \cdot (\text{body weight}/50)$ ; typical value of peripheral volume of distribution =  $623 \cdot (\text{body weight}/50)$ ; typical value of intercompartmental clearance =  $34.3 \cdot (\text{body weight}/50)^{3/4}$ .

<sup>b</sup> The relative standard errors for bootstrap estimates reported as standard error/median.

<sup>c</sup> For interindividual and interoccasion variability terms, the relative standard errors are given for the corresponding variance term.

<sup>d</sup> Eta shrinkage, 40%.

<sup>e</sup> Eta shrinkage, 22%.

<sup>f</sup> Eta shrinkage, 49%.

<sup>g</sup> One extreme bootstrap estimate (85,500) was excluded; inclusion of this value produces a bootstrap median of 642 (relative standard error, 540%).

weight and HIV status. IIV terms were included on the absorption rate coefficient, CL/ $F$ , and the mean transit time, and an IOV term was included on CL/ $F$ . Residual variability was modeled using combined additive and proportional error terms. The parameter estimates are presented in Table 2, together with the results from the bootstrap.

The initial inclusion of allometrically scaled body weight with fixed exponents on all volume and clearance terms resulted in a drop in OFV of 24 units ( $P < 0.001$ ) and body weight was retained in the model. In the univariate evaluation of covariate relationships, age, serum creatinine concentration, creatinine clearance, alkaline phosphatase concentration (log transformed), and mean corpuscular volume were statistically significant ( $P < 0.05$ , with descending significance in the order written). Age, serum creatinine concentration, and alkaline phosphatase concentration were still in the model following the forward search, but none remained after the backward deletion step. Finally, presence of HIV was found to be a borderline statistically significant covariate on bioavailability (it decreased bioavailability by 15.4%;  $P = 0.0068$ ). Refinement of the variance models resulted in IIV on only a few parameters, and CL/ $F$  showed a high degree of IOV.

Both the population predicted values and the individual predictions described the observed concentrations well, and no trends were seen in plots of the absolute individual weighted residuals versus the individual predictions (Fig. 2). Shrinkage in residual error (epsilon shrinkage) was low (12%), signifying that goodness-of-fit plots involving individual predictions are

adequate. Stratifying the plots by study location, dose level, HIV status, creatinine clearance concentration, and occasion did not reveal any deviations in any of the strata (data not shown). The descriptive and predictive properties of the model are further illustrated in Fig. 3, in which the results from the VPC are presented stratified by study location.

The model by Peloquin et al. (27) resulted in underprediction of EMB concentrations in general. The same was true for the model by Zhu et al. (39), particularly at about the time for peak concentrations. Introduction of allometric scaling by body weight led to better agreement but with the same trends overall (Fig. 4). The simulations should be interpreted only with respect to the general tendency, since the variability terms in the models were from our model.

### DISCUSSION

The pharmacokinetic features of EMB in South African tuberculosis patients were best described using a two-compartment model with first-order absorption preceded by a transit compartment. The large study sample ( $n = 189$  in total, whereof 129 had a rich sampling schedule) ensures a thorough covariate search over the distributions of evaluated factors and low imprecision in parameter estimates, with the exception of a few variability terms.

The application of a two-compartment model is in agreement with the findings among healthy North American subjects (27) and the early studies by Lee et al. (18, 19), whereas Zhu et al. (39) applied a one-compartment model. Absorption has been described to be a first-order process (39) or with a model including lag time and zero-order absorption (27) in previous work. The variable absorption of EMB has been hypothesized to be due to binding or chelation in the gastrointestinal tract and suggested to be described by consecutive absorption processes on the basis of preclinical data (18, 19). Our model does not provide further evidence for the mechanism of the complex absorption but is solely a description, and alternative models applied during model development, e.g., dual absorption sites, could also describe the data reasonably well.

The estimated typical CL/ $F$  of 39.9 liters/h or 0.80 liters/h/kg for the typical individual of 50 kg concurs with the results obtained by Lee et al. (18), in which CL/ $F$  can be approximated to 0.75 liters/h/kg or 44 liters/h in subjects weighing an average of 59 kg. In general, however, the CL/ $F$  estimate is lower than that previously reported (Table 3), including the typical estimates of previous population model analyses (27, 39). Accordingly, the model predictions based on previous models (27, 39) resulted in underprediction of EMB concentrations (Fig. 4). Correcting for body weight reduced the disagreement between observations and predictions slightly, and the differences can thus be attributed partly to differences in body weight in the various study populations, which is also indicated in Table 3. Since the effect of concomitant food consumption on the extent of absorption is negligible (1, 27), administration under fasting conditions, done in our study, is not expected to explain the differences between studies. A higher fraction unbound or malabsorption due to malnourishment would lead to a higher CL/ $F$  when total plasma concentrations are measured and is therefore an unlikely cause for the observed disagreements. Possible factors explaining the divergences may be other dif-

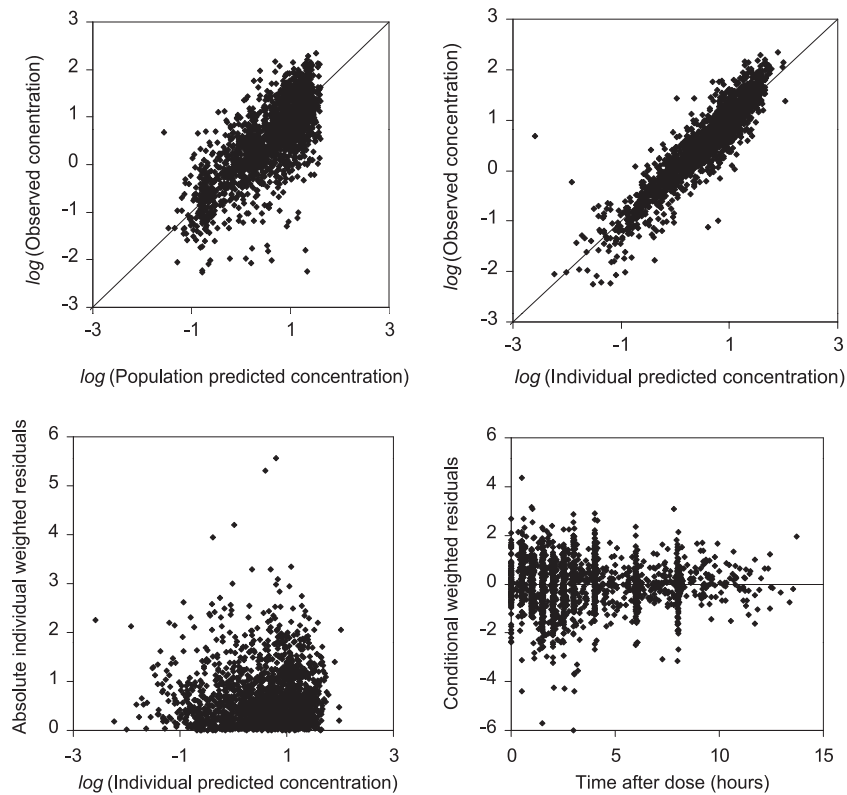


FIG. 2. Goodness-of-fit plots. Observed concentrations versus the population predictions (top left) and individual predictions (top right), in which the solid line represents the line of identity. Absolute individual weighted residuals versus the individual predictions (bottom left) and conditional weighted residuals versus time after dose (bottom right).

ferences in the study population, sampling schedules (time interval, rich versus sparse data), analytical methods, and drug formulations.

Covariate effects were not investigated in previous studies, and in this study two factors were identified. The presence of HIV infection was found to decrease bioavailability by 15%.

The effect was of borderline statistical significance but was included in the model since it is consistent with previous findings that the presence of HIV infection corresponds with reductions in the EMB area under the concentration-time curve (AUC) and maximum concentration in plasma (22, 39) and because low systemic concentrations of antituberculosis drugs

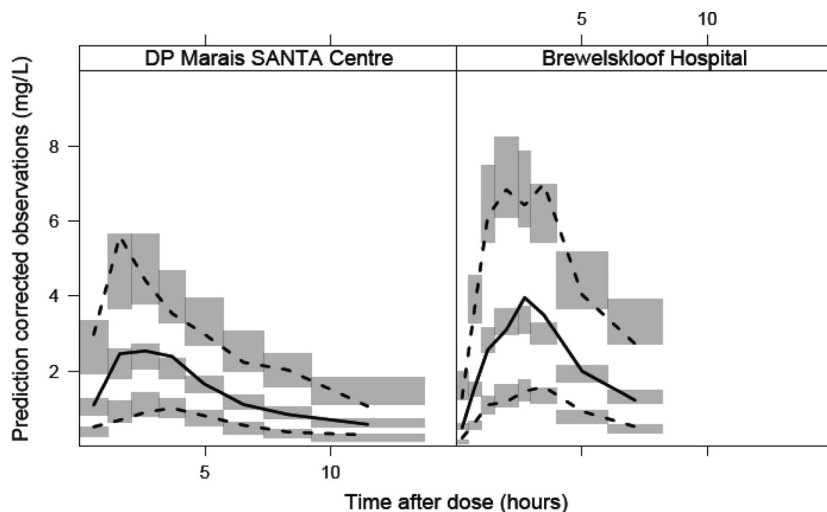


FIG. 3. Results from a visual predictive check ( $n = 1,000$ ) applying population prediction correction. The median and the prediction interval (5th and 95th percentiles) of the observed data are shown as solid and dashed black lines together with the confidence intervals (shaded area) of the corresponding median and prediction interval for the simulated data. The data were binned on the basis of the number of observations.

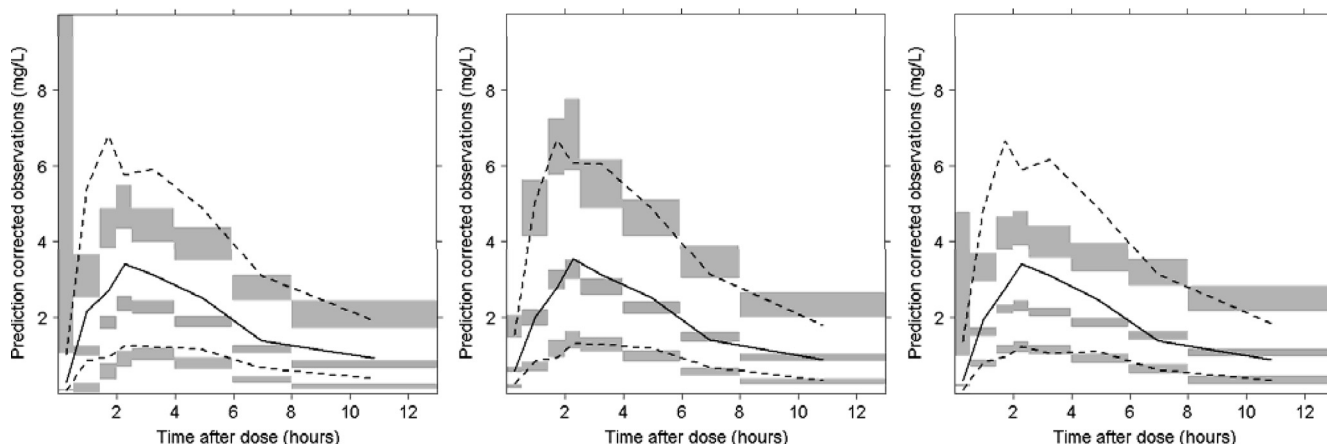


FIG. 4. Predictions by previously published models by means of visual predictive checks ( $n = 200$ ) applying population prediction correction. The dashed and solid lines are the 5th, 50th, and 95th percentiles of the observed data. The confidence interval of the median and the prediction interval (5th and 95th percentiles) for the simulated data are given as the shaded areas. Predictions were obtained by employing the models developed by Pelouquin et al. (27) (left panel), us (27) (middle panel), and Zhu et al. (39) (right panel), modifying the published models by inclusion of allometrically scaled body weight on clearance and volume terms and lending variability terms from our model. Thus, the results of the simulations should mainly be interpreted with respect to the general tendency.

have been reported in HIV-infected patients (26, 28). The effect of body size was modeled by means of allometrically scaled body weight on clearance and volume terms. In our data set, one subject had a BMI above  $30 \text{ kg/m}^2$ , but a proportion had low BMI values (18% had BMIs of  $<16 \text{ kg/m}^2$ ). Taking into account obesity and underweight requires assessment of other size descriptors which better describe body composition, such as BMI or lean body weight. These measures were not assessed in the *scm* procedure due to a high positive correlation ( $r \geq 0.80$ ) with body weight. As a control of this approach,

an alternative model with BMI related to  $CL/F$ , in addition to the final model, was tested but did not improve the outcome.

A large proportion of the patients were classified as being severely malnourished, which may cause malabsorption, reduced drug metabolism and excretion, and decreased binding to plasma proteins (23, 24). If plasma protein binding is altered, the interpretation of the effects on elimination capacity using measurements of total plasma concentrations is complicated since an increased fraction unbound results in the estimation of increased clearance on the basis of total plasma

TABLE 3. Previously reported values of oral clearance of ethambutol<sup>a</sup>

$CL/F$ (liters/h)	$CL/F$ (liters/h/kg)	Population	Dosing and sampling	Comments	Reference
40.3	0.81	Adults with tuberculosis; body wt, 47 kg	800, 1,000, or 1,200 mg daily doses; predose and rich and sparse sampling to 8-12 h postdose		Present study
67, 53	1.05, 0.83	Adults with tuberculosis; body wt, 63.5 kg	800 mg, single and daily doses; predose and rich sampling to 12 h postdose	Values refer to data following first and repeated doses, respectively	13
43, 44	0.73, 0.75	Healthy adults; body wt, 59 kg	15 mg/kg, single dose; rich sampling to 24 h postdose	$CL/F$ estimated from individual AUCs and doses; values refer to 2 oral formulations, respectively	18
70	Not estimated	Adults with tuberculosis; body wt not reported	25 mg/kg, daily doses; predose and rich sampling to 8 h postdose	AUC reported; $CL/F$ roughly estimated using mean value of AUC and dose	22
90	1.14	Healthy adults; body wt, 79.3 kg	25 mg/kg, single dose; rich sampling to 48 h postdose	Values reported refer to model-based analysis	27
55	1.17	Adults with tuberculosis; body wt, 47.3 kg	750 mg, daily doses; predose and rich sampling to 12 h postdose	AUC reported; $CL/F$ roughly estimated using mean values of AUC, dose, and body wt	30
74, 86	1.10, 1.42	Adults with tuberculosis; body wt, 64 kg	1,325 mg, daily doses; predose and rich sampling to 10 h postdose	Values reported refer to noncompartmental and model-based analyses, respectively	39

<sup>a</sup>  $CL/F$ , body weight, and doses are the reported means in the studied populations. Values in italics were not reported in the publications but have been estimated given mean values of AUC, dose, and/or body weight, unless stated otherwise.

concentrations and may mask an unchanged or decreased elimination capacity. This is of particular importance for drugs highly bound to plasma proteins. Studies of the effect of nutritional status on the pharmacokinetics of the tuberculosis drugs are rare (29). Since EMB is mainly excreted unchanged via the kidneys and has low plasma protein binding (20 to 30% bound), the effect of an increased unbound fraction is, however, not anticipated to markedly affect  $CL/F$  estimated using total concentrations. Indeed, EMB concentrations in children with tuberculosis were found not to be affected by malnutrition (11). Furthermore, the model in which an effect of BMI on the final model was evaluated did not identify a statistically significant effect on  $CL/F$  by malnourishment, i.e., that a low BMI would be associated with a higher  $CL/F$ .

Renal excretion is the primary elimination pathway for EMB, and lengthening of the dose interval or reduction of the dose is recommended in impaired renal function (17, 38). Few patients with renal impairment were included; only 8 patients had creatinine clearances of <50 ml/min, and 2 of them had creatinine clearances of <30 ml/min. This could, in part, explain that the covariate search did not identify a relationship with renal function markers. In addition, the initial inclusion of body weight as a covariate in conjunction with a positive correlation between body weight and creatinine clearance makes the effect of renal function difficult to distinguish from the effect of body weight. The effect of renal impairment on EMB exposure has not been extensively investigated previously, but a study in 13 hospitalized patients with stable renal failure (creatinine clearance range, 5 to 81 ml/min) reported clearance and renal clearance to range from 12 to 37 liters/h and 0.36 to 3.6 liters/h, respectively, following intravenous administration of EMB (33), implying a low contribution of renal elimination in these patients, but a direct comparison with normal renal function was not available. Accordingly, further studies are needed to simultaneously evaluate the elimination of EMB in subjects with normal and impaired renal function.

Interindividual variability terms were not possible to estimate for all parameters. For example, IIV was assessed for  $F$ , but this estimate tended to converge toward 0, and the only disposition parameter with an associated variability term is  $CL/F$ . The model with IOV on  $CL/F$  was highly statistically significant and was chosen, although a model with IOV on  $F$  tended to result in a lower OFV but did not terminate successfully. Thus, the IOV on  $CL/F$  probably describes interoccasion variability in the systemic exposure related to the absorption/bioavailability rather than the elimination, but it was not possible to capture this adequately. It should be noted that the estimate of the interoccasion variability exceeded the interindividual variability. This observation indicates that the usefulness of individualized treatment employing therapeutic drug monitoring may be limited for EMB.

One future use of this model may be the prediction of systemic exposure in children. The task of establishing an appropriate dosage in children is complicated by the fact that target exposure in the pediatric population is not defined, but the present pediatric dose recommendations by WHO are based on a review of the clinical experience in children. In view of the lack of ocular toxicity in children of all ages receiving EMB at doses from 15 to 30 mg/kg, daily doses of 20 mg/kg

(range, 15 to 25 mg/kg) and intermittent doses of 30 mg/kg three times weekly to children of all ages are recommended (10, 37). At present, our model has the ability to predict disposition by taking changes due to body size and presence of HIV infection into account. Optimally, elimination would be described with a model where the processes involved, i.e., glomerular filtration and active secretion, are described and that also includes the dependence on body size, maturation, and organ function. The present data available in children imply that apart from body size-related changes in disposition, bioavailability appears to be lowered in children due to reduced absorption (11, 39). All these aspects need consideration for adequate forecasting of EMB exposure in children.

In summary, the population pharmacokinetics of EMB were described in South African patients with pulmonary tuberculosis. Our estimate of  $CL/F$  was lower than that reported previously, a finding that can partly be explained by the differences in body weight between the studied populations. The interoccasion variability in  $CL/F$  exceeded the interindividual variability. The decrease in bioavailability in the presence of HIV coinfection is consistent with earlier findings. Renal function could not be identified as a covariate on clearance, potentially due to the limited number of patients with renal impairment.

#### ACKNOWLEDGMENTS

This study was funded by the Medical Research Council of South Africa, the National Research Foundation of South Africa, and the Swedish International Development Agency. Helen Melleron received partial support from European and Developing Countries Clinical Trials Partnership and training through grants from the Fogarty International Center (U2RTW007370/3 and 5U2RTW007373).

Justin Wilkins was an employee of Novartis Pharma AG from December 2006 to November 2010 and is currently an employee of Exrimo NV, with neither employment producing a conflict of interest.

#### REFERENCES

1. Ameer, B., R. E. Polk, B. J. Kline, and J. P. Grisafe. 1982. Effect of food on ethambutol absorption. *Clin. Pharm.* **1**:156–158.
2. American Thoracic Society/Centers for Disease Control and Prevention/Infectious Diseases Society of America. 2003. Treatment of tuberculosis. *Am. J. Respir. Crit. Care Med.* **167**:603–662.
3. Anderson, B. J., and N. H. G. Holford. 2009. Mechanistic basis of using body size and maturation to predict clearance in humans. *Drug Metab. Pharmacokinet.* **24**:25–36.
4. Beal, S. L., L. B. Sheiner, and A. J. Boeckmann. 1989–2006. NONMEM user's guides. Icon Development Solutions, Ellicott City, MD.
5. Bergstrand, M., A. C. Hooker, J. E. Wallin, and M. O. Karlsson. 2011. Prediction corrected visual predictive checks for diagnosing nonlinear mixed-effects models. *AAPS J.* **13**:143–151.
6. Breda, M., et al. 1999. Effect of rifabutin on ethambutol pharmacokinetics in healthy volunteers. *Pharmacol. Res.* **40**:351–356.
7. Chideya, S., et al. 2009. Isoniazid, rifampin, ethambutol, and pyrazinamide pharmacokinetics and treatment outcomes among a predominantly HIV-infected cohort of adults with tuberculosis from Botswana. *Clin. Infect. Dis.* **48**:1685–1694.
8. Cockcroft, D. W., and M. H. Gault. 1976. Prediction of creatinine clearance from serum creatinine. *Nephron* **16**:31–41.
9. Conte, J. E., Jr., E. Lin, Y. Zhao, and E. Zurlinden. 2002. A high-pressure liquid chromatographic-tandem mass spectrometric method for the determination of ethambutol in human plasma, bronchoalveolar lavage fluid, and alveolar cells. *J. Chromatogr. Sci.* **40**:113–118.
10. Donald, P. R., D. Maher, J. S. Maritz, and S. Qazi. 2006. Ethambutol dosage for the treatment of children: literature review and recommendations. *Int. J. Tuberc. Lung Dis.* **10**:1318–1330.
11. Graham, S. M., et al. 2006. Low levels of pyrazinamide and ethambutol in children with tuberculosis and impact of age, nutritional status, and human immunodeficiency virus infection. *Antimicrob. Agents Chemother.* **50**:407–413.
12. Holford, N. 2005. The visual predictive check—superiority to standard diagnostic (Rorschach) plots, abstr. 738. Abstr. Population Approach Group in Europe 14. <http://www.page-meeting.org/?abstract=738>.

13. **Israilli, Z. H., C. M. Rogers, and H. El-Attar.** 1987. Pharmacokinetics of antituberculosis drugs in patients. *J. Clin. Pharmacol.* **27**:78–83.
14. **Jonsson, E. N., and M. O. Karlsson.** 1999. Xpose—an S-PLUS based population pharmacokinetic/pharmacodynamic model building aid for NONMEM. *Comput. Methods Programs Biomed.* **58**:51–64.
15. **Karlsson, M. O., and L. B. Sheiner.** 1993. The importance of modeling interoccasion variability in population pharmacokinetic analyses. *J. Pharmacokinet. Biopharm.* **21**:735–750.
16. **Karlsson, M. O., and N. Holford.** 2008. A tutorial on visual predictive checks, abstr 1434. *Abstr. Population Approach Group in Europe 17.* <http://www.page-meeting.org/?abstract=1434>.
17. **Launay-Vacher, V., H. Izzedine, and G. Deray.** 2005. Pharmacokinetic considerations in the treatment of tuberculosis in patients with renal failure. *Clin. Pharmacokinet.* **44**:221–235.
18. **Lee, C. S., J. G. Gambertoglio, D. C. Brater, and L. Z. Benet.** 1977. Kinetics of oral ethambutol in the normal subject. *Clin. Pharmacol. Ther.* **22**:615–621.
19. **Lee, C. S., D. C. Brater, J. G. Gambertoglio, and L. Z. Benet.** 1980. Disposition of ethambutol in man. *J. Pharmacokinet. Biopharm.* **8**:335–346.
20. **Lindbom, L., J. Ribbing, and E. N. Jonsson.** 2004. Perl-speaks-NONMEM (PsN)—a Perl module for NONMEM related programming. *Comput. Methods Programs Biomed.* **75**:85–94.
21. **Lindbom, L., P. Pihlgren, and E. N. Jonsson.** 2005. PsN-Toolkit—a collection of computer intensive statistical methods for non-linear mixed effect modeling using NONMEM. *Comput. Methods Programs Biomed.* **79**:241–257.
22. **McIlleron, H., et al.** 2006. Determinants of rifampin, isoniazid, pyrazinamide, and ethambutol pharmacokinetics in a cohort of tuberculosis patients. *Antimicrob. Agents Chemother.* **50**:1170–1177.
23. **Murry, D. J., L. Riva, and D. G. Poplack.** 1998. Impact of nutrition on pharmacokinetics of anti-neoplastic agents. *Int. J. Cancer Suppl.* **11**:48–51.
24. **Oshikoya K. A., H. M. Sammons, and I. Choonara.** 2010. A systematic review of pharmacokinetics studies in children with protein-energy malnutrition. *Eur. J. Clin. Pharmacol.* **66**:1025–1035.
25. **Peets, E. A., W. M. Sweeney, V. A. Place, and D. A. Buyske.** 1965. The absorption, excretion, and metabolic fate of ethambutol in man. *Am. Rev. Respir. Dis.* **91**:51–58.
26. **Peloquin, C. A., et al.** 1996. Low antituberculosis drug concentrations in patients with AIDS. *Ann. Pharmacother.* **30**:919–925.
27. **Peloquin, C. A., et al.** 1999. Pharmacokinetics of ethambutol under fasting conditions, with food, and with antacids. *Antimicrob. Agents Chemother.* **43**:568–572.
28. **Perlman, D. C., et al.** 2005. The clinical pharmacokinetics of rifampin and ethambutol in HIV-infected persons with tuberculosis. *Clin. Infect. Dis.* **41**:1638–1647.
29. **Ramachandran, G., A. K. Kumar, and S. Swaminathan.** 2011. Pharmacokinetics of anti-tuberculosis drugs in children. *Indian J. Pediatr.* **78**:435–442.
30. **Ruslami, R., et al.** 2010. Pharmacokinetics of antituberculosis drugs in pulmonary tuberculosis patients with type 2 diabetes. *Antimicrob. Agents Chemother.* **54**:1068–1074.
31. **Savic, R. M., D. M. Jonker, T. Kerbusch, and M. O. Karlsson.** 2007. Implementation of a transit compartment model for describing drug absorption in pharmacokinetic studies. *J. Pharmacokinet. Pharmacodyn.* **34**:711–726.
32. **Savic, R. M., and M. O. Karlsson.** 2009. Importance of shrinkage in empirical Bayes estimates for diagnostics: problems and solutions. *AAPS J.* **11**:558–569.
33. **Varughese, A., D. C. Brater, L. Z. Benet, and C. S. Lee.** 1986. Ethambutol kinetics in patients with impaired renal function. *Am. Rev. Respir. Dis.* **134**:34–38.
34. **West, G. B., J. H. Brown, and B. J. Enquist.** 1997. A general model for the origin of allometric scaling laws in biology. *Science* **276**:122–126.
35. **West, G. B., J. H. Brown, and B. J. Enquist.** 1999. The fourth dimension of life: fractal geometry and allometric scaling of organisms. *Science* **284**:1677–1679.
36. **Wilkins, J. J., et al.** 2008. Population pharmacokinetics of rifampin in pulmonary tuberculosis patients, including a semimechanistic model to describe variable absorption. *Antimicrob. Agents Chemother.* **52**:2138–2148.
37. **World Health Organization.** 2006. Ethambutol efficacy and toxicity: literature review and recommendations for daily and intermittent dosage in children. World Health Organization, Geneva, Switzerland.
38. **World Health Organization.** 2010. Treatment of tuberculosis: guidelines, 4th ed. World Health Organization, Geneva, Switzerland.
39. **Zhu, M., et al.** 2004. Pharmacokinetics of ethambutol in children and adults with tuberculosis. *Int. J. Tuberc. Lung Dis.* **8**:1360–1367.